On the Electrical Properties of Synthetic Manganocolumbite $MnNb_2O_{6-\delta}$

Flaviano García-Alvarado,*,† Alodia Orera,† Jesús Canales-Vázquez,‡ and John T. S. Irvine‡

Departamento de Química, Universidad San Pablo-CEU, Urbanización Montepríncipe, 28668-Boadilla del Monte, Madrid, Spain, and Centre for Advanced Materials, School of Chemistry, University of St. Andrews, North Haugh, St. Andrews, Fife KY16 9ST, Scotland, United Kingdom

Received February 8, 2006. Revised Manuscript Received June 1, 2006

A manganocolumbite with nominal composition $MnNb_2O_6$ has been prepared under air in order to characterize its electrical behavior. Although powder X-ray diffraction indicates the presence of a single phase, electrical and microscopic characterization reveals two different bulk responses. The origin of these two bulk elements seems to relate to the presence of two compositions with slight excess of either manganese or niobium. These are stabilized instead of $MnNb_2O_6$, indicating the instability of the nominal composition. However, these variations of composition are not large enough to be detected by our structural characterization methods, although the effect is easily detected by impedance spectroscopy and from particle shape in scanning electron microscopy (SEM). Under reducing conditions, monophasic samples with Nb/Mn ratio close to 2 are obtained. From magnetic measurements the main magnetic contribution is determined to be from Mn^{2+} in all cases. The oxygen deficiency of reduced $MnNb_2O_{6-\delta}$ was only just determinable by thermogravimetry, indicating that $\delta \sim 0.02$. On annealing at 1150 °C in 5% H_2, a decrease in unit cell volume of 0.22%, an increase in electrical conductivity of 4 orders of magnitude, and the appearance of a Pauli contribution also indicate a small degree of Nb reduction.

Introduction

Columbite is a well-known class of mineral exhibiting a 3-D framework that is related to the α-PbO_2 structural type. The structure of $MnNb_2O_6$ was described some time ago.[1] Projections of the framework are depicted in Figure 1. Mn and Nb are ordered in an orthorhombic structure, with Mn−O_6 and Nb−O_6 octahedra forming chains along the *c*-axis. The octahedra share edges along the chain, while parallel Mn−O_6 and Nb−O_6 chains alternate along the *b*-axis. In the *ab* plane an interesting topology can be seen. The *a*-axis is the oxygen packing direction along which half of the octahedral sites are occupied, alternating the empty and full half set. While all the occupied sites are Pb sites in α-PbO_2, the sequence Mn−Nb−Nb−Mn−Nb−Nb... is found in the columbite $MnNb_2O_6$. Hence columbite can be considered as a superstructure of α-PbO_2.

The structure is extremely interesting inasmuch as nature has shown that very different type of cations can be distributed and ordered in these two types of octahedra (see for example ref 2 for an updated description of its crystal chemistry). This capability for metal accommodation opens a possibility of tuning some properties through compositional control. Besides, the presence of Nb^{5+} in nominal $MnNb_2O_6$ and the stability of niobium in lower oxidation states may allow the formation of relatively large amounts of anion deficiency under reducing conditions. If such reducing conditions are too extreme, for instance, when Nb or Ta metal are used as oxygen getters, reduction is accompanied by structural changes and the phases $MnNb_2O_{4.33}$ and $MnNb_2O_{3.67}$ are obtained.[3]

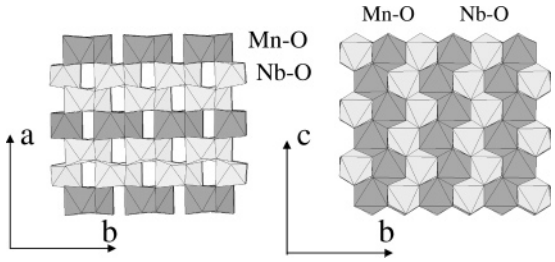

Figure 1. Schematic representation of the columbite structure projected along the *c*-axis (left) and the *a*-axis (right) (adapted from ref 1).

This is the motivation that led us to investigate the electrical properties of ceramics crystallizing with the aforementioned structure. This first work is devoted to $MnNb_2O_6$, which is apparently a simple case where Mn and Nb are expected in the 2+ and 5+ oxidation state, respectively. We are presenting the electrical behavior of both nominal $MnNb_2O_6$ and a reduced sample, $MnNb_2O_{6-\delta}$.

Other physical properties have been previously investigated for different members of the columbite family.[1,4,5] In particular, the magnetic properties are of interest since this structural type allows cooperative interaction between magnetic ions as reported in the case of $MnNb_2O_6$[1] and more recently in a new member of the columbite family, $CuNb_2O_6$.[5]

* Corresponding author: telephone 34 1 372 4728; fax 34 1 351 0496; e-mail flaga@ceu.es.
† Universidad San Pablo-CEU.
‡ University of St Andrews.

(1) Weitzel, H. *Z. Anorg. Allg. Chem.* **1971**, *380*, 119.
(2) dos Santos, C. A.; Zawislak, L. I.; Kinast, E. J.; Antonietti, V.; da Cunha, J. B. M. *Braz. J. Phys.* **2001**, *31*, 616.
(3) Chumarev, V. M.; Mar'evich, V. P.; Pakratov, A. A. *Inorg. Mater.* **2003**, *39*, 285.
(4) Eibschutz, M. *Phys. Rev.* **1967**, *156*, 259.
(5) Drew, M. G. B. *J. Mater. Chem.* **1993**, *3*, 889.

10.1021/cm0603203 CCC: $33.50
Published on Web 07/06/2006

Experimental Section

The synthesis of manganocolumbite was carried out by solid-state reaction of a 1:1 mixture of predried $MnCO_3$ and Nb_2O_5. After the reagents were ground with acetone, the mixture was pressed into pellets and slowly heated to 800 °C. The temperature was then held for a couple of hours to ensure decomposition of the carbonate as thermogravimetric analysis, performed in a TGA 1000M+ apparatus (Fine Work Co. Ltd.), showed that this process is completed at 560 °C. Afterward the temperature was increased up to 1050 °C at 1 °C/min and kept there for 20 h. After being reground and pressed into pellets, the product was fired again at 1050 °C for a further 15 h, to achieve homogeneity. Three different samples were afterward obtained from the as-prepared manganocolumbite by three different thermal treatments for the sintering step. In all cases the product was pressed into pellets with a saturated water solution of poly(vinyl alcohol) as binder. Afterward, pellets were heated at 2 °C/min up to 800 °C to decompose and eliminate the binder. A first sample was obtained by sintering pellets at 1150 °C for 16 h. A second sample was prepared by sintering at the same temperature but for a longer period of time (48 h). A third sample was sintered at 1150 °C under reducing conditions with a flow of H_2/Ar (5%) for 20 h.

X-ray diffraction (XRD) data were collected in transmission mode with a Stoe StadiP X-ray diffractometer, with Cu $K\alpha_1$ radiation in the range $2\theta = 5-80°$ in steps of 0.5° at 300 s/step. XRD data were indexed by a least-squares procedure. The microstructure was investigated with a JEOL-JSM-5600 scanning microscope equipped with an Oxford Link detector to perform energy-dispersion spectroscopy (EDS) analysis. Selected area electron diffraction (SAED) and high-resolution transmission electron microscopy (HRTEM) were performed on a JEOL JEM 2011 electron microscope equipped with a ±20° double-tilt sample holder, operating at 200 kV. The equipment was also fitted with an Oxford Link detector to perform EDS analysis. Samples for TEM work were prepared by dispersion of fine ground material onto a perforated carbon film supported on a Cu grid. The variation of the magnetic susceptibility was recorded on a Quantum Design's magnetic property measurement system (MPMS−SQUID) in the 2−300 K temperature range. The applied field was 1000 Oe. Impedance spectroscopy was performed with a FRA Solartron 1260 in the 1 MHz−0.1 Hz range over the temperature range 25−800 °C. Measurements were carried out on pellets coated with either gold or silver paste, which act as electrodes. In the case of the sample sintered under H_2/Ar (5%), the same atmosphere was used for electrical measurements.

Results and Discussion

X-ray diffraction experiments showed that the synthesis performed at 1050 °C yielded crystalline compounds. The corresponding diffraction pattern can be fully indexed on the basis of the well-known columbite $MnNb_2O_6$. After the sample was sintered at 1150 °C, we did not detect any significant change in the diffraction pattern, indicating no change in the crystallographic nature of the samples. Regarding cell size, nominal $MnNb_2O_6$ sintered under air exhibits the following cell parameters: $a = 14.4587(8)$ Å, $b = 5.7740(3)$ Å, and $c = 5.0919(3)$ Å, while when the sintering occurs under H_2 (5%) the obtained parameters are $a = 14.4459(11)$ Å, $b = 5.7703(4)$ Å, and $c = 5.0880(5)$ Å. Besides the unit cell decrease and slight changes of intensities for some reflections, no other differences were found between the sample sintered under air and the sample sintered under H_2 (5%). Reduction decreases the unit cell volume by about 0.22%. The oxygen deficiency of reduced $MnNb_2O_{6-\delta}$ was only just determinable by thermogravimetry, indicating that $\delta \sim 0.02$ at 900 °C under H_2 (5%). For most transition metal oxides, volume increases on reduction; however, this is not the case for d^0 species such as Nb^{5+} and Ti^{4+}, where a very small degree of reduction creates a significant decrease in unit cell size due to a change in the nature of bonding. This reduction can be viewed as introducing electrons into the conduction band and hence leading to a degree of metallic bonding. This effect counterbalances the limited intrinsic expulsion ongoing from a d^0 to a d^1 oxide. Similar effects have previously been observed in fluorite, perovskite, and ramsdellite lattices (see for example ref 6).

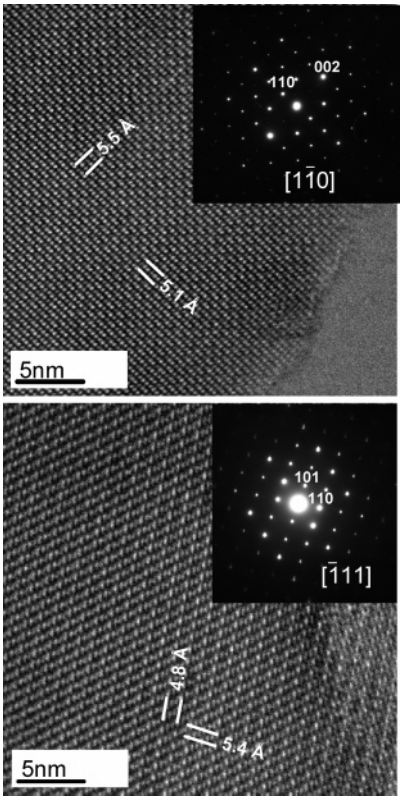

Figure 2. Selected area electron diffraction patterns of reduced "$MnNb_2O_6$" along several zone axes and corresponding high-resolution images.

The microstructural study made by TEM revealed that neither local ordering nor superstructure is introduced on reduction. Figure 2 shows typical electron diffraction patterns and high-resolution images obtained from crystals belonging to the sample reduced under 5% H_2. Patterns can be fully indexed by use of the columbite cell obtained by XRD. For the nonreduced sample, exactly the same types of SAED and HRTEM images have been recorded. We have not found any difference between these two samples, apart from relative stability of crystals under the beam. While the reduced sample is very stable, the unreduced $MnNb_2O_6$ seems to be affected, most probably reduced, by the beam.

The first results discussed regarding the electrical properties correspond to the sample obtained by sintering the manganocolumbite at 1150 °C for 16 h. The relative density

(6) Canales-Vázquez, J.; Ruiz-Morales, J. C.; Irvine, J. T. S.; Zhou, W. *J. Electrochem. Soc.* **2005**, *152*, A1458.

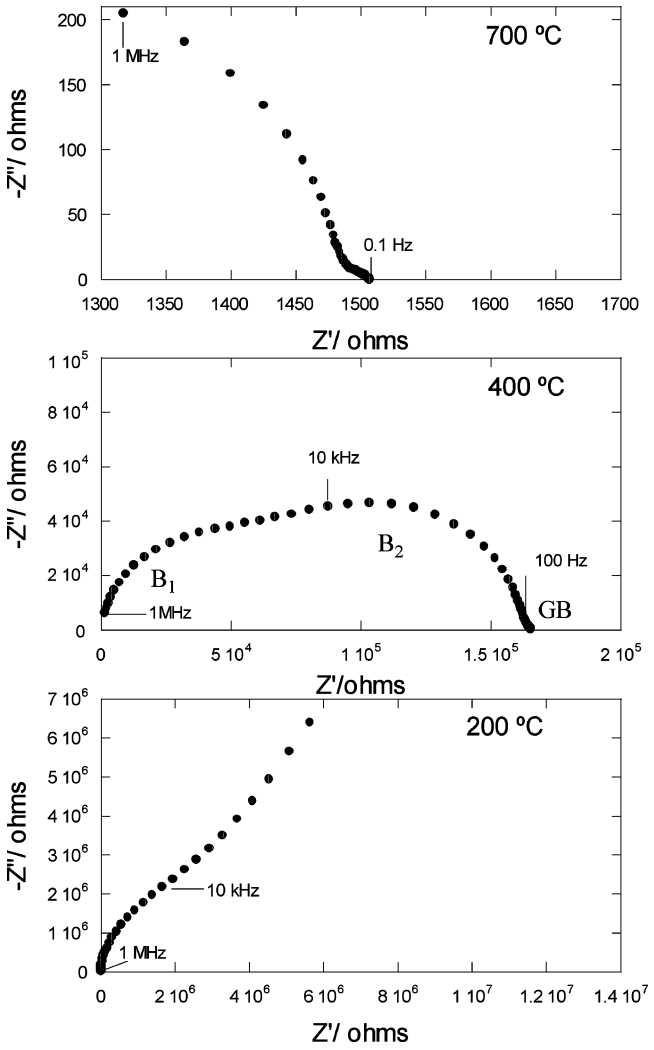

Figure 3. Typical impedance data presented in the $Z''-Z'$ plane for pelletized "$MnNb_2O_6$" sintered at 1150 °C/16 h. Spectra shown were recorded at 700, 400, and 200 °C.

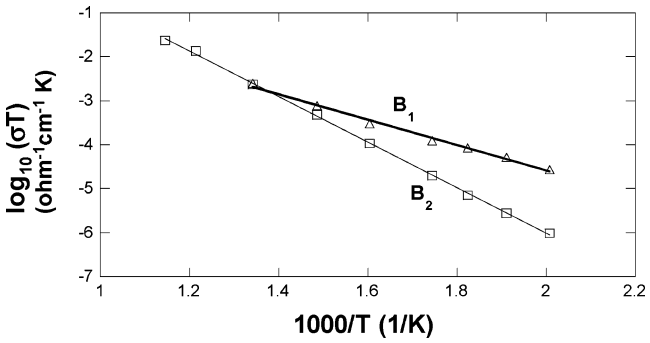

Figure 4. Arrhenius plot for pelletized "$MnNb_2O_6$" sintered at 1150 °C/16 h showing the temperature dependence of conductivity for two different bulks, B_1 and B_2.

of the sample was close to 76%. Some attempts were made to prepare denser pellets of $MnNb_2O_6$ by sintering at 1200 °C. However, a decrease in the relative density to 68% was observed. Therefore, pellets obtained at 1150 °C were chosen to perform the comparative study presented below between nonreduced and reduced $MnNb_2O_6$.

Typical impedance plots are shown in Figure 3. At 400 °C, the corresponding Nyquist plot reveals the existence of at least three different semicircles that can be associated with as many electrochemical responses. After appropriate correction of the experimental setup contribution, the responses were considered as three RCPE elements in series, where CPE represents constant phase elements used as an alternative to pure capacitors due to the presence of depressed arcs. The "true capacitances" can be extracted from the so-called pseudo-capacitance (Q) through the very well-known relationship $C = R^{(1-n)/n}Q^{1/n}$, where R is the resistance and n is an exponent indicating the degree of deviation from the ideal pure capacitor behavior, or in other words n indicates a frequency distribution. The capacitance associated with the highest frequency semicircle is approximately 1.9×10^{-12} F/cm with the n value close to 1, which clearly indicates that it is due to a bulk contribution.[7] This may also be the case of the intermediate frequency arc since the corresponding capacitance value, although 1 order of magnitude larger (2.6×10^{-11} F/cm with n close to 1), may also be indicative of a bulk-type contribution. The capacitance value might indicate that this bulk response is due to the presence of a secondary phase. However, X-ray diffraction experiments did not detect such a second phase. Another possibility is that this second semicircle could be due to a constriction-type grain boundary, but as we will see below SEM data will rule this out and confirm two types of bulk crystal. We will refer to these two contributions hereafter as bulk contributions B_1 and B_2. Finally, at low frequency we can observe (see Figure 3, 700 °C) a semicircle that is highly depressed. The complex fitting at different temperatures yielded values ranging from 4.4×10^{-8} to 5.6×10^{-9} F/cm with n values of around 0.5. The presence of this semicircle cannot be unambiguously assigned to a grain boundary contribution due to the fact that fitted data are associated with a significant error in the low-frequency part of the spectra due to the large impedance elements at lower frequency. We performed some other experiments with a different metal electrode (i.e., silver) and the spectra obtained were similar. This seems to indicate that the low-frequency part of the spectrum shown in Figure 3 (top) is not dominated by the electrode response.

As a general comment on the results presented in Figure 3, one could say that the electrical resistance is controlled by bulk resistances. As expected, the high-frequency semicircle is still visible at low temperatures (see for example data obtained at 200 °C) while the low-frequency semicircle is better defined at higher temperatures (700 °C).

The temperature dependence of both B_1 and B_2 conductivities is shown in the Arrhenius plots depicted in Figure 4. Both B_1 and B_2 follow linear behavior in the temperature ranges where the resistance values extracted from the complex fitting are reliable. B_1 is associated with an activation energy (0.57 eV) smaller than that corresponding to B_2 (0.97 eV). As a consequence of such different activation energies, a crossover appears at relatively low temperatures (close to 470 °C). The fact that the total conductivity is dominated by B_2 at high temperatures as well as low temperatures, despite an anticipated crossover, demonstrates the occurrence of parallel conduction paths with an effective

(7) Irvine, J. T. S.; Sinclair, D. C.; West, A. R. *Adv. Mater.* **1990**, *2*, 132.

short circuit through the small grained phase (see below) at high temperatures. At lower temperatures current would flow more easily through B_1, while at higher temperatures the easiest bulk path would be through B_2. The circuit model could perhaps be refined to allow for the combined series and parallel elements; however, there is insufficient differentiation between the element responses, especially at the grain boundaries, to allow a more complex model to be refined without introducing unacceptable errors. The total conductivity values presented later are of course reliable in any event. The poor definition of the low-frequency response (grain boundary), also prevented good-quality data about its activation energy being obtained. However, the grain boundaries do not have a strong influence on the total resistance, at least at high temperature, since the resistance associated with this response is quite low (see Figure 3, 400 and 700 °C).

We now pay attention to the presence of two bulks even though the characterization made by powder X-ray diffraction indicated that the prepared manganocolumbite is single-phase. For this purpose, Figure 5a shows the morphology of one face of the electrically characterized pellet as seen by scanning electron microscopy. Two different types of grains are clearly detected, at least according to particle size and morphology. Energy dispersive analysis indicated that both types of crystals contain Nb and Mn in ratios that are never very far from nominal (2:1). However, the possibility of having a phase of variable composition cannot be excluded. We have to note that the average size of crystals is in the range 4−7 μm for one type, the largest and loosest crystals, but this value becomes close to 1−1.5 μm, for the other type, the smallest and agglomerated. This is an important limitation when thinking on the EDS results since, for example, the penetration depth of the X-ray used to record the EDS spectra at 20 kV is close to 3 μm for a density of about 4.5 g cm^{-3}. In our case, with experimental densities even smaller (3.5−3.8 g cm^{-3}), we have to be aware that analysis of crystals is affected by the presence of other crystals that are underneath. This is a very well-known limitation of the EDS technique when used on a pelletized sample, but it is especially important when small variations of composition are expected in small crystals.[8] When this limitation is taken into account, our EDS results just indicate that the composition of the sample is not far from homogeneity, but still a tendency of the largest crystals to have a slight excess of niobium has been detected. Accordingly, the small crystals seem to have a slight excess of manganese. We have also analyzed a crushed sample by EDS but by use of a transmission electron microscope. Preparation by crushing pellets to obtain powder avoids the above-mentioned limitation as a thin crystal method is used.[9] Nevertheless, it introduces a limitation as particle size is modified during preparation of sample for observation. However, a reliable conclusion was obtained. We have confirmed that large crystals (5−10 μm) have a niobium excess. The average Nb/Mn ratio found was ca. 2.37. Assuming that stoichiometry

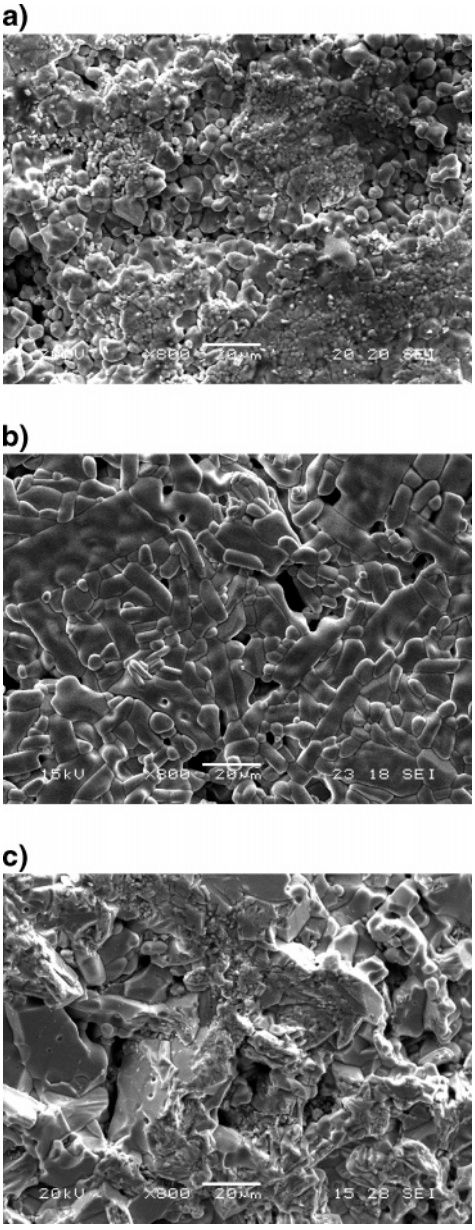

Figure 5. SEM images of (a) pellet face of "$MnNb_2O_6$" sintered at 1150 °C/16 h, (b) pellet face of $MnNb_2O_6$ sintered at 1150 °C/48 h, and (c) pellet cross section of $MnNb_2O_6$ sintered at 1150 °C/48 h.

is maintained in these large crystals, the corresponding formula is $Mn_{0.9}Nb_{2.1}O_6$. On the other hand, two different sets of small crystals are found regarding their Nb/Mn ratios. One set has a clear low Nb/Mn ratio, ca. 1.80, while for the other set the ratio is the same as for large crystals. These latter crystals are likely to arise from grinding large crystals, while the first set correlates with the small crystals observed by SEM in the prepared pellet (see Figure 5a). For these, if one assumes again that stoichiometry is kept, the composition would be $Mn_{1.1}Nb_{1.9}O_6$. Therefore, to have an average composition of $MnNb_2O_6$, the ratio between $Mn_{0.9}Nb_{2.1}O_6$ and $Mn_{1.1}Nb_{1.9}O_6$ is calculated to be 80:20.

It is very important to mention that such variation of composition has a strong influence in both morphology and electrical properties. Hence results may be pointing to a tendency of the metals to adopt oxidation states different from Mn^{2+} and possibly Nb^{5+}, which correspond to nominal and stoichiometric composition $MnNb_2O_6$.

(8) Goodhew, P. J.; Humphreys, F. J. *Electron Microscopy and Analysis*; Taylor and Francis Ltd.; London, 1988.
(9) Cliff, G.; Lorimer, G. W. *J. Microsc.* **1975**, *103*, 203.

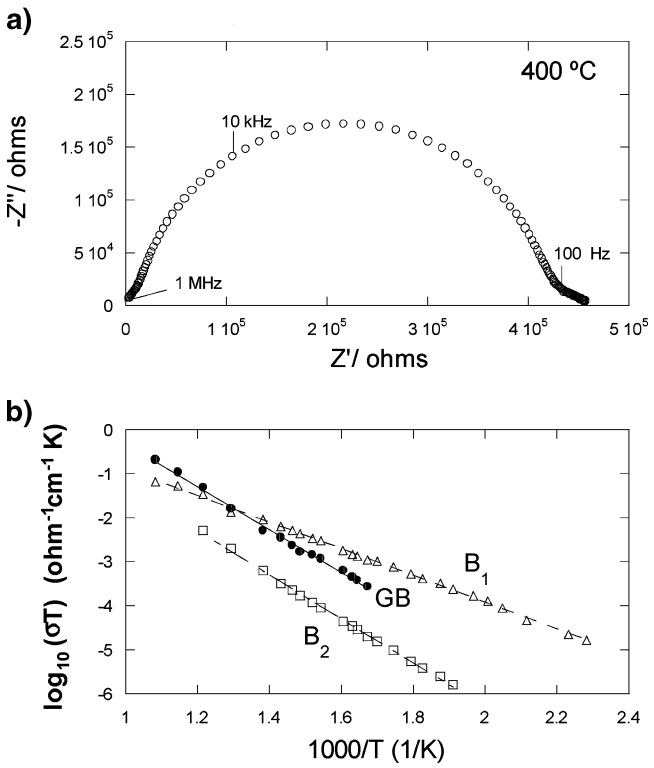

Figure 6. (a) Typical impedance data presented in the $Z''-Z'$ plane for pelletized "$MnNb_2O_6$" sintered at 1150 °C/48 h. Spectrum was recorded at 400 °C. (b) Arrhenius plot for pelletized $MnNb_2O_6$ sintered at 1150 °C/48 h showing the temperature dependence of conductivity for two different bulks, B_1 and B_2, and grain boundary, GB.

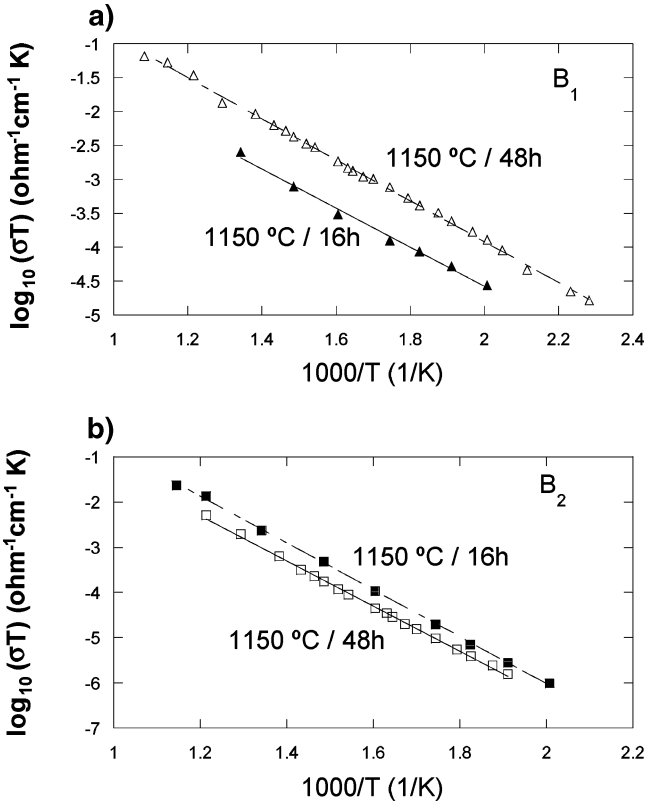

Figure 7. Arrhenius plot showing the temperature dependence of conductivity of bulks B_1 and B_2 for two different sintering times (16 and 48 h): (a) B_1; (b) B_2.

Since this lack of homogeneity in the cationic distribution could be due just to slow kinetics of reaction between the reagents, we have studied another sample that was treated at the same temperature but three times longer, that is, at 1150 °C for 48 h. The relative density, 78%, was only enhanced by 2% with respect to the previous treatment. Nevertheless, the effect of the different thermal history on electrical properties, composition, and morphology has also been evaluated.

The top-view SEM shown in Figure 5b shows that a different morphology of the pellets has been produced. Although a higher dispersion of particle sizes is observed, it is very important to note that the 1 μm crystals have disappeared. A cross-section SEM image, presented in Figure 5c, shows that in fact the big plates are composed by crystals of different morphology where microcrystals are still present, though in a smaller amount. Energy dispersion spectroscopy indicates still the presence of two compositions. Nothing could be concluded regarding the evolution of composition of crystals but that large crystals have slightly evolved toward nominal composition $MnNb_2O_6$.

In agreement with the morphological and chemical characterization, we still found that the electrical response is due to the contribution of two different bulks and grain boundary elements. A first difference is that the grain boundary contribution can be analyzed now in more detail, and hence fitting of data produced reliable results regarding the origin of this element. Besides, B_1 and B_2 relative resistances have changed. This can be seen clearly in Figure 6a, which shows a typical impedance plot at 400 °C if compared with the equivalent data showed in Figure 3. The high-frequency arc of Figure 6a is due to a bulk response ($C = 1.85 \times 10^{-12}$ F/cm, $E_a = 0.60$ eV)) and this is also the case of the intermediate frequency semiarc ($C = 5.62 \times 10^{-12}$ F/cm, $E_a = 1.03$). And finally the low-frequency semiarc ($C = 1.2 \times 10^{-8}$ F/cm, $E_a = 0.99$ eV) corresponds to grain boundary contribution. The Arrhenius behavior of the three contributions detected by ac impedance can be seen in Figure 6b. It can be seen that the high resistance of B_2 dominates the electrical behavior for almost the whole range of temperature investigated. Resistance is dominated by B_2 at all temperatures.

The phase diagram of the binary system $MnO-Nb_2O_5$ was reported a long time ago.[10,11] Only the 1:1 phase, that is, $MnNb_2O_6$, has been detected between MnO and Nb_2O_5. However, our results seem to point to the existence of other stable phases, especially under nonreducing conditions. This is why we have started a new study exploring the solid solution between MnO and Nb_2O_5 and its defect chemistry. Results will be reported elsewhere.

It is interesting to note now that conductivity of the bulk with the smallest capacitance, B_1, increases when the thermal treatment is longer, while in the case of the bulk with larger capacitance, B_2, the conductivity decreases despite a decrease in capacitance (Figure 7). The evolution in capacitance behavior is consistent with the evolution of microstructure observed in Figure 5. B_1 grains become larger and more

(10) Robert, S. R., Ed. *Phase Equilibria Diagrams: Volume XI*; American Ceramic Society: Westerville, OH, 1995.
(11) Han, H.; Lin, Q.; Wei, S. K. *Chin. J. Met. Sci. Technol.* **1990**, *6*, 98.

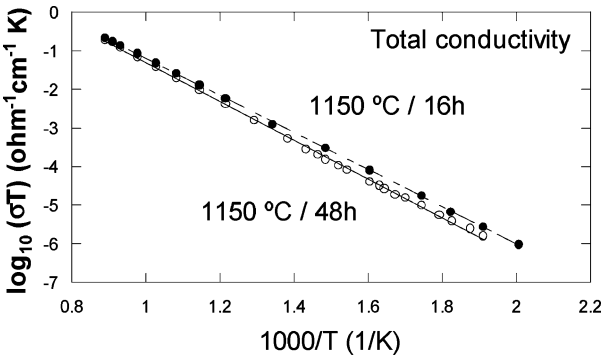

Figure 8. Arrhenius plot showing the total conductivity of "$MnNb_2O_6$" pelletized at 1150 °C for two different sintering times (16 and 48 h).

isolated, B_2 grains become more continuous through the microstructure, and hence the conduction pathway becomes essentially series-dominated. The net result is that the overall conductivity does not change strongly with thermal treatment (Figure 8).

In view of all data shown above, it is now surprising that X-ray diffraction experiments show the existence of just one single phase. The difference in compositions detected by EDS ($Mn_{0.9}Nb_{2.1}O_6$ and $Mn_{1.1}Nb_{1.9}O_6$) does not seem to be enough to induce a change in the long-range crystallographic unit cell that is determined through conventional XRD. Still, the existence of two bulk electrical responses seems to be related with two different phases. The different compositions of the two phases are enough to produce bulks with different electrical properties. Large crystals, that is, those presenting a manganese deficiency ($Mn_{0.9}Nb_{2.1}O_6$), are expected to contain Mn in the lowest oxidation state (i.e., Mn^{2+}). Note that interstitial oxygen is not likely to be allowed in this structure to compensate the excess of cations with very high oxidation states (Nb^{5+} and Nb^{4+}). On the contrary, small crystals, having a deficiency of niobium, may allow the presence of both Mn^{2+} and Mn^{3+}. Both extreme situations should have an influence on the electrical properties, and thus two different electrical behaviors can be justified.

The existence of two polymorphs coexisting in columbites has been previously reported in $CuNb_2O_6$.[5,12] $CuNb_2O_6$ forms an orthorhombic columbite phase at temperatures above 1000 °C. At lower temperatures (ca. 700 °C), however, although the unit cell parameters are almost unchanged, the symmetry is lower, rendering a monoclinic cell ($\beta = 91.8°$) with much smaller particle size. There may be a similar situation for $MnNb_2O_6$. Nevertheless, if a very weak monoclinic distortion was present, it would be difficult to detect the two different phases, unless higher resolution techniques were used. From our data we cannot say that such a monoclinic phase does coexist with the orthorhombic columbite.

Using the aforementioned thoughts about oxidation states as hypothesis, we suppose that our nominal $MnNb_2O_6$, contains a certain ratio of Mn-rich and Mn-poor phases that evolves very slowly because of its dependence upon the oxygen partial pressure. Only a change in this parameter may allow a fast change of composition and ratio of both types of crystals. It was for this reason that we sintered a pellet of

(12) Wahlstrom, E.; Marinder, B. O. *Inorg. Nucl. Chem. Lett.* **1997**, *13*, 559.

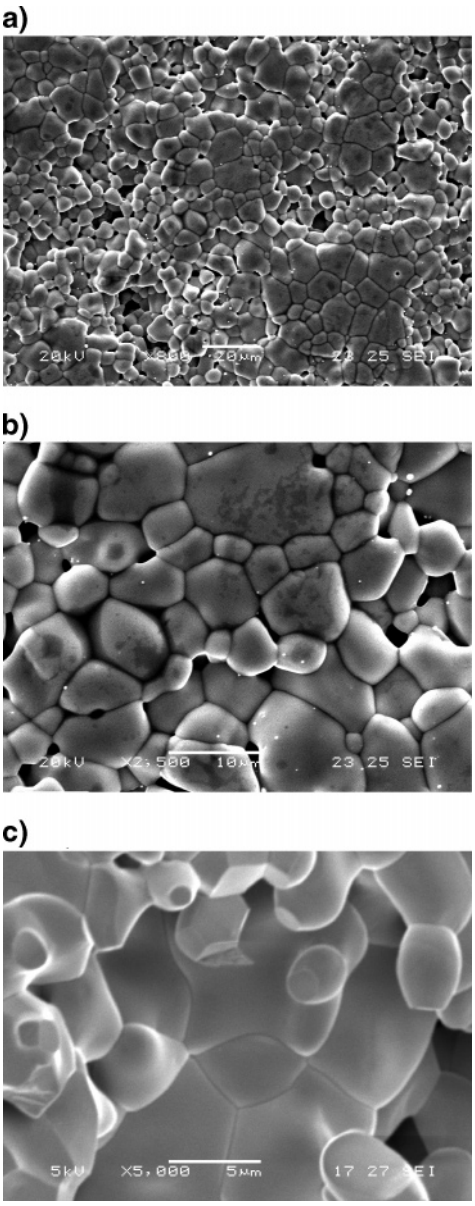

Figure 9. SEM images of "$MnNb_2O_6$" sintered at 1150 °C/20 h under 5% H_2: (a) pellet face; (b) larger magnification of pellet face; (c) pellet cross section.

nominal $MnNb_2O_6$ under 5% hydrogen for not too long a time (20 h) and at the same temperature used for samples described above (1150 °C). After this treatment a relative density of ca. 80% was obtained. Although this value is somewhat similar to those obtained for the samples sintered under air, the subsequent results help to clarify many of the points raised above.

Figure 9 shows several SEM images of a pellet annealed under 5% H_2. The surface image is presented in Figure 9a. If it is compared with the surface shown in Figure 5a, we can deduce that this is quite homogeneous since mainly one type of crystal is observed. Only very small and scattered submicrometric crystals (white spots) can be observed besides the main type of crystals. Figure 9b shows a magnification for a better visualization of such submicrometric crystals. EDS analysis reveals that these crystals have a Nb/Mn ratio of 1.6. They are the very scarce remnants of the Mn-rich phase. On the other hand, the main type of

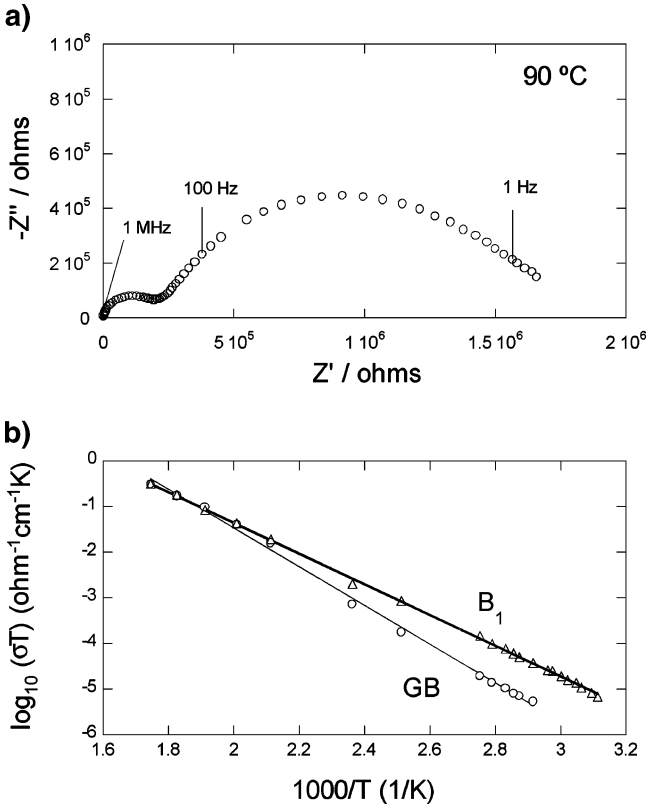

Figure 10. (a) Typical impedance data presented in the $Z''-Z'$ plane for pelletized "$MnNb_2O_6$" sintered at 1150 °C/20 h under 5% H_2. Spectrum was recorded at 90 °C. (b) Arrhenius plot showing the temperature dependence of conductivity for bulk, B_1, and grain boundary, GB.

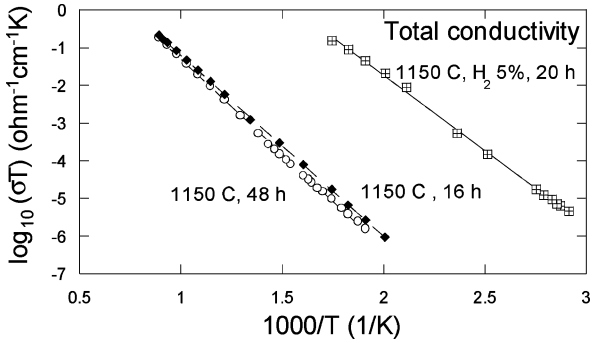

Figure 11. Arrhenius plot showing the temperature dependence of total conductivity of "$MnNb_2O_6$" for two different sintering times under air (16 and 48 h) and reducing conditions (5% H_2, 20 h).

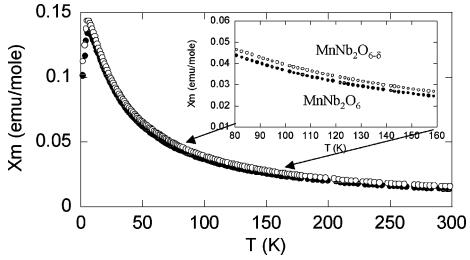

Figure 12. Magnetic susceptibility of both nominal "$MnNb_2O_6$" (1150 °C under air) and reduced $MnNb_2O_{6-\delta}$ (1150 °C, 5% H_2) versus temperature in the range 4.2−300 K. The inset shows a selected temperature range allowing a better visualization of Pauli contribution in the reduced sample.

crystals should belong to the Nb-rich phase, but as it has grown at the expense of Mn-rich phase, the final composition is now less rich in niobium and hence closer to nominal (Nb/Mn = 2.1; within the experimental error this is $MnNb_2O_6$). A cross section of the same pellet is presented in Figure 9c. As can be seen, it shows the same morphological characteristics. This sample can be considered as a single phase with nonvariable composition.

In accordance with this observation and since the presence of the Mn-rich phase is negligible, impedance spectra (see Figure 10a) show only two semicircles. The high-frequency semicircle is interpreted as coming from a bulk with a capacitance of 2.74×10^{-12} F/cm. From the Arrhenius behavior shown in Figure 10b, an activation energy of 0.66 eV is calculated. Both capacitance and activation energy seems to indicate that this bulk is related to what we have termed B_1, while B_2 is not present. From the second semiarc a capacitance of 8.24×10^{-10} F/cm and an activation energy of 0.84 eV can be calculated. We assign this semiarc to the grain boundary response.

We come back now to those samples presented previously that were prepared and sintered in static air. Two bulk responses were detected and now we can say that B_1, with the lower activation energy, is assigned to a Nb-rich phase, whereas B_2, with higher activation energy, is assigned to a Mn-rich phase.

On the basis of EDS analysis, we can say that in samples prepared and sintered in static air the two average compositions $Mn_{0.9}Nb_{2.1}O_6$ and $Mn_{1.1}Nb_{1.9}O_6$ exist, while if sintering is carried out under very reducing conditions the sample is homogeneous with a composition of $MnNb_2O_6$.

The drastic influence of the atmosphere on phase homogeneity is likely to be related to the presence of Mn^{3+} in the Nb-deficient compound. Reducing conditions may favor reduction of Mn^{3+} to Mn^{2+} and hence formation of $Mn^{2+}(Nb^{5+})_2O_6$. Oxidizing conditions favor the formation of Mn^{3+} and hence the observed compositional segregation.

Total conductivity is also drastically affected by reduction, as can be seen in Figure 11. This shows Arrhenius behavior for the three samples analyzed in this work. A change of more than 4 orders of magnitude is observed when $MnNb_2O_6$ is treated under H_2 (5%) at 1150 °C. This strong change may point to the further reduction of $Mn^{2+}(Nb^{5+})_2O_6$ to $Mn^{2+}(Nb^{5+})_{2-x}(Nb^{4+})_xO_{6-x/2}$, although thermal analysis does indicate that x is very small.

To investigate the possible presence of Nb^{4+}, we have performed magnetic measurements. Magnetic susceptibility as a function of temperature over the wide range 4.2−300 K is shown in Figure 12 for both the sample sintered in air and the sample sintered in H_2 (5%). The same general behavior has been found. At low temperature the presence of cooperative effects can be observed. A maximum in the χ_m versus temperature curve indicates that an antiferromagnetic interaction dominates at very low temperatures: T_N = 6.3 and 6.0 K for the sample sintered in air and in reducing conditions, respectively. According to these values, it seems that this interaction is not affected by reduction. The existence of antiferromagnetism in $MnNb_2O_6$ columbite is very well reported[1,13,14] since even the antiferromagnetic

(13) Klein, S.; Weitzel, H. *Acta Crystallogr. A* **1976**, *32*, 587.
(14) Nielsen, O. V.; Lebech, B.; Larsen, F. K.; Holmes, L. M.; Ballman, A. A. *J. Phys. C: Solid State Phys.* **1976**, *9*, 2401.

structure has been determined by neutron diffraction of single crystals.

For the $MnNb_2O_6$ sintered in air, the Curie−Weiss law is obeyed between temperatures just above the maximum and room temperature (RT). Between 6 K and RT the obtained Weiss constant is −20.5 K while the Curie constant is 4.37. The effective magnetic moment calculated for free ions is $5.91\mu_B$, which agrees with a high-spin 5 e^- system expected for the formulation $Mn^{2+}(Nb^{5+})_2O_6$. However, note that for this sample two different average compositions have been detected: $Mn_{0.9}Nb_{2.1}O_6$ and $Mn_{1.1}Nb_{1.9}O_6$. For both of them the main contribution is arising from the presence of large quantities of Mn^{2+}, as their compositions are close to the ideal $MnNb_2O_6$.

Regarding the reduced sample, the treatment under a reducing atmosphere provokes an increase in the magnetic susceptibility (see Figure 12). Above T_N this increase has been found to be constant, indicating the contribution of Pauli paramagnetism ($\chi_p \sim 2.24 \times 10^{-3}$ emu/mole). The Curie paramagnetic contribution has been calculated to be identical to that of the nonreduced sample, corresponding again mainly to the presence of a high-spin 5 e^- system. It is interesting to note that while we have found evidence of the reduction of Nb^{5+} from the existence of Pauli paramagnetism, thermogravimetric experiments showed that oxygen deficiency is small and close to the resolution of the instrument, pointing to a very low Nb^{4+} concentration. However, the production of few delocalized electrons upon a small degree of Nb reduction has a drastic effect in conductivity, which has been determined to change by 4 orders of magnitude.

Conclusions

A manganocolumbite with nominal composition $MnNb_2O_6$ has been prepared in order to characterize its electrical behavior. Although the samples were considered as XRD single-phase, electrical and microscopic characterization reveals the presence of two different bulks. The origin of these two bulks seems to be the intrinsic instability of the nominal composition prepared under air. Indeed, it seems that compositions with slight excess of either manganese or niobium are stabilized. These variations of composition are not large enough to be detected by our structural characterization methods; however, they do have an influence on the electrical response. This is because the variation of composition may be accompanied by a change in the oxidation states of manganese. Under reducing conditions, monophasic samples can be obtained with Nb/Mn ratio close to 2. Much higher conductivity than in nominal $MnNb_2O_6$ has been found for this reduced $MnNb_2O_{6-\delta}$ columbite due to the production of delocalized electrons upon a small degree of Nb reduction.

Acknowledgment. We thank The Royal Society for funding the Spain−U.K. Joint Project Grant 2004−2006 and EPSRC for platform grant. F.G and A.O. also acknowledge the financial support received from the Ministerio de Educación y Ciencia (Grant MAT2004-03070-C05-01) and Universidad San Pablo CEU. We are also indebted to our colleagues J.C. Ruiz Morales, J. Romero, and U. Amador for helpful discussions.

CM0603203